

## HELICOPTER MAIN ROTOR DYNAMIC PROPERTIES IDENTIFICATION USING FULL SCALE GROUND AND FLIGHT TESTS MEASUREMENTS

Jacek Matecki  
 "PZL-Świdnik" S.A. Leonardo Helicopters Company Świdnik, Poland  
 E-Mail: jacek.matecki@leonardocompany.com  
 Phone: +48 81 722 6332

### Abstract

The one of the key challenges during new rotor blades design is the proper tuning of their dynamic properties. The specific design stages are defined as milestones and each particular stage needs specific methodology for a correct identification of the rotor dynamics. Every stage needs validated tools for a correct rotor characteristic frequencies prediction, which finally will be observed on the helicopter during normal helicopter operations. In this paper the review of estimation methodologies for the helicopter main rotor dynamic properties is presented with their application to new, improved W-3A Sokol helicopter MR blade set during design stage stand tests and during full scale helicopter on ground and in flight tests campaign.

### 1. SYMBOLS AND ABBREVIATIONS

CFD	Computational Fluid Dynamics
CG	Center of Gravity
CMIF	Complex Mode Indicator Function
DFT	Digital Fourier Transform
$E_i$	Bending stiffness of the blade segment $i$
FAR	Federal Aviation Regulations
FEM	Finite Element Method
FRF	Frequency Response Function
$G_i$	Torsional stiffness of the blade segment $i$
$h_i$	horizontal type blade mode with nodes number $i$
IGE	In Ground Effect
MAC	Modal Assurance Criterion
MR	Main Rotor
$N_r$	Main rotor speed relative to nominal speed [%]
PZL	Polish Aviation Works (Państwowe Zakłady Lotnicze)
$t_i$	torsional type blade mode with nodes number $i$
TR	Tail Rotor
$v_i$	vertical type blade mode with nodes number $i$

Symbols are declared in body text.

### 2. INTRODUCTION

The PZL W-3A Sokol helicopter is the compliant with FAR-29 airworthiness requirements version of the PZL W-3 helicopter. The dedicated program for helicopter performance improvement was raised by PZL. The development of new MR blade was significant part of it. New blade was designed using new geometry shape, new family of airfoils, new composite materials and manufacturing technology. Due to significant number of improvements planned for new MR blade design the full range of optimization analyses were performed to ensure proper rotor dynamic properties. The significant

decision which has impact on the project was future interchangeability between old and new blades. It imposes set of limitations required to be met for new design. From other side, the several known data for helicopter could be used during design stage.

The three significant stages were defined during development process of the new blade:

- Design stage including overall geometry shape optimization and internal structure definition, the dynamic properties optimization was part of the activity;
- Ground testing stage dedicated to the first verification of strength and dynamic properties of specimens and first produced examples of new blades, performed in laboratory test stands'
- Testing on the helicopter, including first runs of new rotor and rotor flutter stability tests performed on tied down helicopter on ground followed by first on ground and in flight tests on prototype helicopter.

Present paper shows step by step methodology used to ensure proper rotor dynamics for new developed rotor. Presented results are compilation of several elder blade projects where methodology was tested.

### 3. DESIGN STAGE – PRELIMINARY AND TECHNICAL DESIGN STEPS

Design stage of the new MR blade development combines methods to fulfil set of desired requirements in helicopter performance and flight properties together with strength, aeromechanical stability of the rotor. Most of these properties fulfilment requires correct placement of main rotor characteristic modes vs. existing on helicopter excitation frequencies.

Following previous company experience in rotor blade design, the coupled methodology using FEM models and internally developed software based on Myklestad method was used to determine rotor dynamics. The operation diagram scheme is presented in Figure 1.

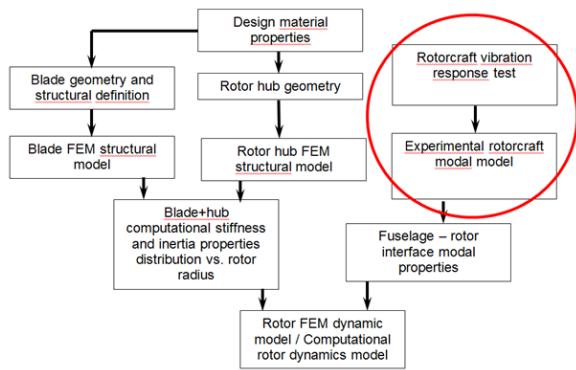


Figure 1. The operation diagram used for determination of the PZL W-3A MR dynamic properties with new blade. The possibility to retrieve structural dynamics from tests due to new blade application on existing helicopter (part inside red circle)

First of all the set of detailed FEM models of the blade segments were built to obtain stiffness and inertia properties distribution along the blade. It allows to determine effects of design details on data values and to check the strength of the blade. Example of detailed model of mid part of the blade is presented on Figure 2.



Figure 2. FEM model of the new MR blade mid part.

The detailed data of the MR hub were taken from kinematic model and from FEM model of the blade grip. Overview of the model is presented on Figure 3.

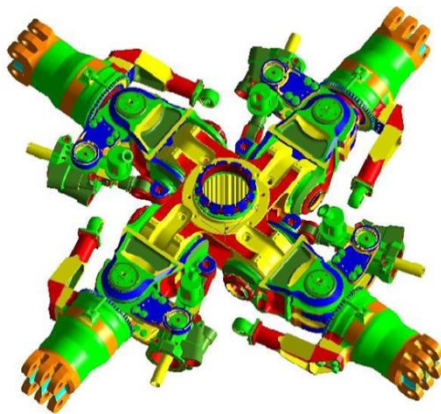


Figure 3 Kinematic model of the PZL W-3A MR hub.

Final results of the detailed FEM models analyzes were the distribution of hub / blade stiffness, shear center position, weight, CG position and moments of inertia. Example beamwise stiffness distribution along the radius is presented in Figure 4.

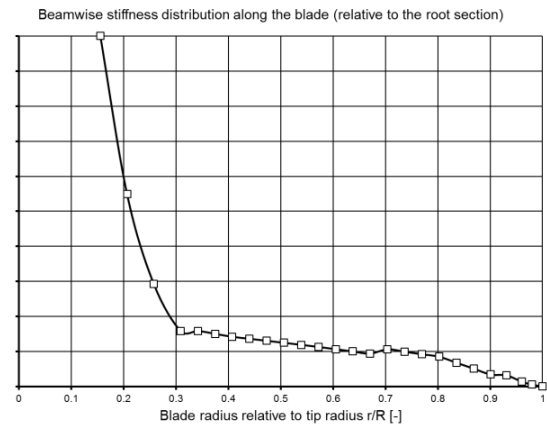


Figure 4. Normalized beamwise stiffness distribution obtained by analysis of the FEM model

Parallel to the hub and blade properties the determination of the helicopter fuselage dynamic properties was performed. Due to required interchangeability of new and old blade, the existing data obtained during PZL W-3A helicopter experimental modal tests were valid. Ground modal tests were made on hanged by MR hub center helicopter fuselage during development stage of the rotorcraft. General layout of the test is presented on Figure 5.



Figure 5. General layout of the PZL W-3A helicopter modal tests.

Results of the tests were obtained as set of characteristic helicopter frequencies and modes. Example mode visualization is presented in Figure 6.

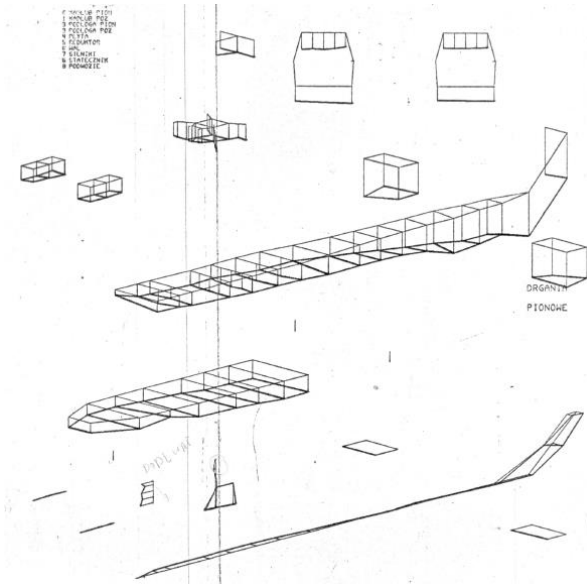


Figure 6. Example of PZL W-3A fuselage characteristic vibration mode obtained by experimental modal test.

Data measured during modal tests were reduced to the top of the MR shaft as set of modal mass/damping/stiffness properties symbolized fuselage – rotor coupling.

The two methods of MR dynamics determination were considered to be finally used for new MR blade development program:

- PZL company developed computer program based on Myklestad analysis method published in [1], used for previous blade design activity;
- Dedicated FEM model built for MR dynamic properties, analyzed by FEM commercial code considered as new approach with potentially wider further possibility to use (coupled analysis with fuselage structural FEM model and FSI calculations was considered in the future).

Both methods used discretized data of stiffness/inertia properties distribution prepared by analysis of detailed FEM models. Main principals of FEM model could be summarized as:

- Blade was modelled as a series of flexible beams with predefined stiffness in beamwise, chordwise and torsional directions and shear center offsets;
- Inertia properties were imposed via lumped mass elements located in the section CGs and connected to the beam with rigid elements;
- Hub was modelled with flexible beams with revolute joints corresponding to horizontal and vertical hinges and pitch horn;
- Boundary conditions at the center of hub are represented by a set of springs and/or imposed displacements constraints depending on the vibration case under investigation.

Schematic sketch of the blade model used is presented in Figure 7.

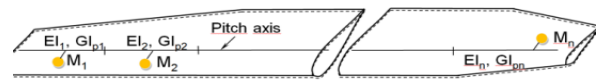


Figure 7. Scheme of blade model used to obtain MR blades dynamic properties.

The identification of mode type calculated by FEM method was performed by calculation of effective mass belongs to the particular mode for selected vibration direction (beamwise, chordwise and torsional):

- (1)  $M_{ei} = \frac{\gamma_i^2}{\{\varphi\}_i^T [M] \{\varphi\}_i}$  - effective mass for mode i;
- (2)  $\gamma_i = \{\varphi\}_i^T [M] \{D\}$  - modal participation factor for mode i;
- (3)  $\{\varphi\}_i^T [M] \{\varphi\}_i$  - generalized mass for mode i

Where:

$\{\varphi\}_i$  - eigenvector normalized (generalized mass is unity  $\{\varphi\}_i^T [M] \{\varphi\}_i = 1$ )

$[M]$  - mass matrix;

$\{D\}$  - vector describing excitation direction;

The algorithm used to identify mode type is presented on Figure 8. Three types of modes: vertical, horizontal and torsional was counted which represents dominated vibration channel of particular mode.

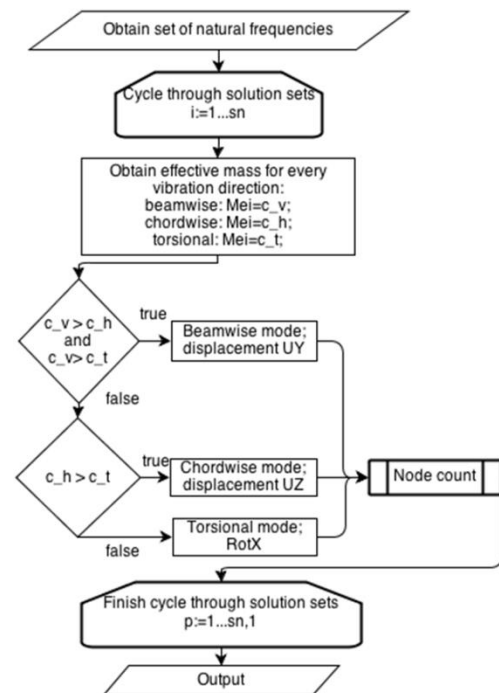


Figure 8. Algorithm used for mode type identification from set of nodes retrieved by FEM MR blade model analysis.

The results of both type analyses are presented as classical Campbell diagram as function of frequencies vs. MR speed  $N_r$  and as set of normalized modes distribution vs. blade radius. The corresponding to the

mode shapes load components distribution is also obtained for every mode.

Example set of results are presented on figure 9 and Figure 10.

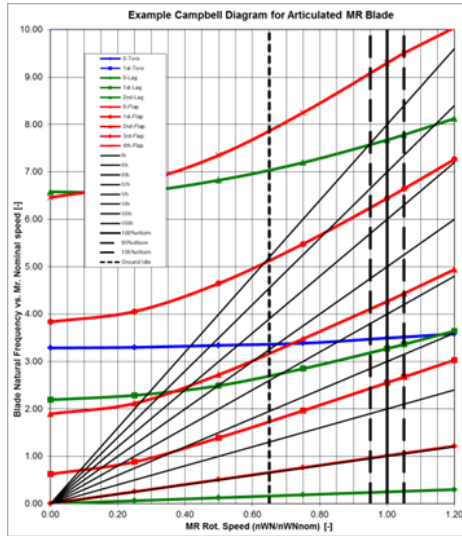


Figure 9. Example Campbell diagram obtained by Myklestad analysis.

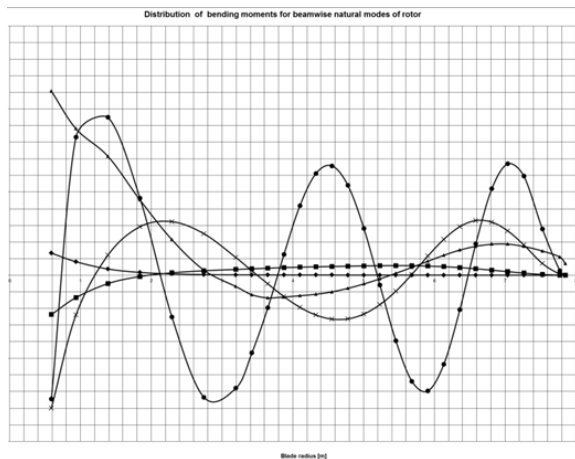


Figure 10. Example set of beamwise moment distribution vs. blade radius corresponding to the normalized mode shapes obtained by Myklestad analysis.

The comparison between frequencies obtained by Myklestad analysis and FEM model analysis was made and is presented in Table 1.

Results comparison FEM-Myklestad	
v1	-4.93%
v2	-1.00%
v3	2.21%
v4	2.33%
v5	3.97%
v6	4.01%
v7	5.00%
h1	-7.95%

h2	-4.56%
h3	-4.61%
t0	-1.33%
t1	-1.19%
t2	-2.17%

Table 1. Comparison of the frequencies obtained by Myklestad and FEM model analyzes for Nr=100% (first FEM model loop).

Together with frequency comparison, the mode vectors were compared using MAC. Results of comparison is presented in Figure 11.

$$(4) \text{MAC}_{XY} = \frac{|\{\varphi\}_X^T \{\varphi\}_Y|^2}{(\{\varphi\}_X^T \{\varphi\}_X)(\{\varphi\}_Y^T \{\varphi\}_Y)} - \text{MAC for two modal vectors X and Y}$$

		FEM analysis results												
		1	2	3	4	5	6	7	8	9	10	11	12	13
Myklestad analysis results	v1	0.95	0.10	0.01	0.06	0.00	0.02	0.03	0.05	0.35	0.03	0.00	0.16	0.00
	v2	0.11	0.98	0.01	0.02	0.11	0.00	0.01	0.06	0.16	0.05	0.00	0.16	0.00
	h1	0.01	0.00	0.99	0.00	0.01	0.07	0.03	0.00	0.03	0.00	0.00	0.02	0.00
	t0	0.01	0.06	0.02	0.96	0.03	0.01	0.02	0.02	0.00	0.03	0.00	0.01	0.00
	v3	0.01	0.14	0.00	0.00	0.98	0.05	0.07	0.01	0.02	0.10	0.00	0.07	0.00
	v4	0.07	0.02	0.00	0.01	0.16	0.51	0.52	0.18	0.20	0.02	0.00	0.07	0.00
	h2	0.00	0.01	0.12	0.00	0.00	0.45	0.47	0.00	0.02	0.00	0.07	0.00	0.00
	v5	0.07	0.09	0.00	0.03	0.02	0.08	0.15	0.97	0.00	0.13	0.01	0.01	0.00
	t1	0.25	0.09	0.00	0.05	0.09	0.12	0.15	0.00	0.89	0.19	0.01	0.13	0.00
	v6	0.06	0.06	0.00	0.03	0.11	0.01	0.02	0.17	0.08	0.96	0.02	0.04	0.00
	h3	0.00	0.00	0.00	0.00	0.00	0.09	0.06	0.00	0.01	0.01	0.94	0.00	0.00
	v7	0.07	0.10	0.00	0.03	0.06	0.04	0.06	0.04	0.12	0.15	0.00	0.84	0.52
	t2	0.03	0.06	0.00	0.03	0.08	0.06	0.09	0.08	0.05	0.21	0.01	0.64	1.00

Figure 11. graphical presentation of the MAC value comparison between modal vectors obtained by Myklestad and FEM model analyzes for Nr=100% (values: 0 – modes fully orthogonal, 1 – modes identical).

The general comparison between both methods shows generally less than 5% difference in frequencies (except h1 mode). The FEM method retrieves generally higher frequency values for vertical type modes (except first v1 and v2 modes) and lower frequency for horizontal modes. The mode vectors comparison shows high compliance between particular modes except modes v4/h2 which was noted as coupled vertical/horizontal (lead-lag) nodes with similar frequencies.

Because results of comparison did not allow the final judgement, both of them was used parallel up to the comparison with stand test results.

#### 4. GROUND STAND TESTS

The second stage of the new blade project which was used to verify correctness of the blade properties prediction was the stand tests campaign performed on the first examples of the new blade.



The measurements of stiffness distribution along the blades and global inertia properties were performed. One blade was cut into pieces to determine mass properties distribution. Measured values were compared to data predicted from detailed FEM models obtained during previous stage.

The blade properties obtained by tests were used instead of analytical data to repeat calculations of rotor dynamics. Current for this stage operational diagram is presented in Figure 12.

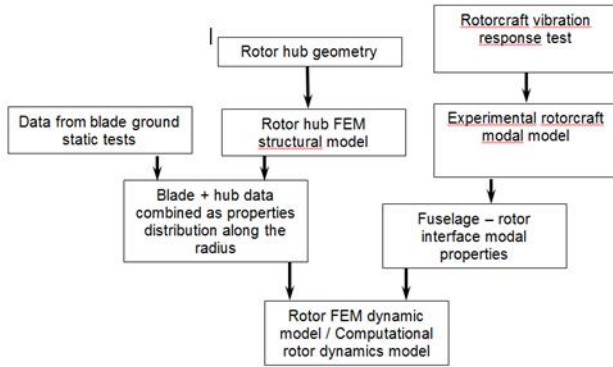


Figure 12. Operational diagram used to obtain rotor dynamic properties after stand tests of first produced blades.

The set of produced blades was designated to the modal tests to obtain characteristic frequencies and corresponding mode shapes. The different blade attachment methods were taken into the consideration for modal testing as vertical hanging, position on flexible ropes, blade pair hanging and cantilever mounting into the wall. Finally the dedicated test stand was used to attach MR blade through hub arm as cantilever beam. This method was used due to existing database of serial blades modal tests performed on these stand. Overall view of the test stand is presented on Figure 13.



Figure 13. General layout of the ground modal test of the new W-3A helicopter MR blades.

During tests the set of modal properties were determined for every produced blade. Example results were presented in Figure 14 and in Figure 15.

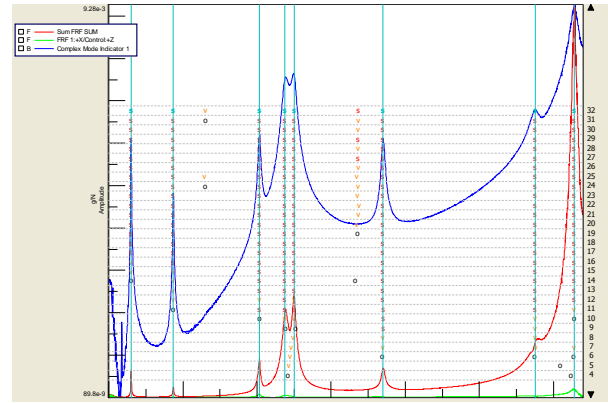


Figure 14. Example FRF, sum of FRF and CMIF functions obtained during ground modal tests.

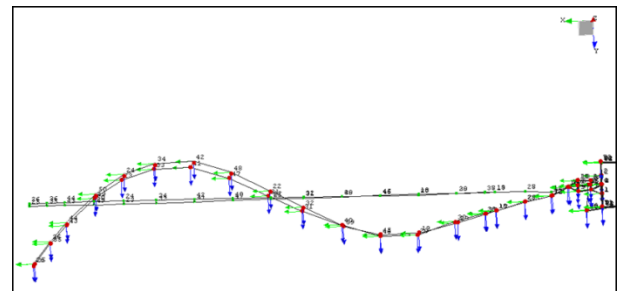


Figure 15. Example mode shape obtained for vertical type mode.

The results of tests were compared with calculations performed by both methods Myklestad and FEM using blade data from static tests and determined by FEM analysis the boundary conditions modeling blade attachment. Comparison between obtained frequencies and measured data was performed and is presented in Table 2.

	Results comparison	
	FEM-Test	Myklestad-Test
v1	-5.99%	1.11%
v2	-1.47%	1.83%
v3	-0.08%	2.21%
v4	3.21%	6.53%
v5	5.14%	10.00%
h0	-0.08%	-4.51%
h1	3.21%	-2.57%
h2	-8.31%	-6.98%
h3	4.72%	-4.80%
t0	2.99%	-0.30%
t1	4.72%	-0.31%
t2	0.00%	-0.03%

Table 2. Comparison of the frequencies obtained by Myklestad, FEM model analyzes and ground stand modal test results (first loop of FEM analyses).

Because of slightly better accuracy in prediction of frequencies and less computational effort the Myklestad method was chosen for future main rotor resonance characteristics analyses of new blades.

## 5. FULL SCALE TESTS ON HELICOPTER

The final stage for the project was the full scale helicopter testing with new MR blades installed. Before first flight the tied down helicopter was used to perform first new blades run.

### 5.1. Blades preparation

Before start of the full scale tests the two selected blades were prepared for measurements by installation of the strain gauges set along each blade. Installed strain gauges were dedicated and scaled to measure beamwise bending (5 stages), chordwise bending (5stages) and torsional moment values (2 stages) along the blade. Schematic position of strain gauges along the blade is presented in Figure 16.



Figure 16. Schematic proposed position of the strain gauges installation along the blade.

Additional measurements were performed on MR hub – beamwise, chordwise moments and pitch control moment on pitch arm.

The measurements in rotating frame were synchronized in time with the same sampling frequency. Data were transmitted to the measurement system together with trigger signal which allows identifying position of selected blade over the helicopter tail boom.

### 5.2. Rotor dynamic motion retrieving from full scale measurements data – general concept

The identification of the rotor dynamics during full scale tests on helicopters allows final verification of the dynamic optimization process and tools validation used to ensure proper placement of the rotor resonance frequencies. Two key phenomena have been used in proposed methodology:

- Resonance of the rotor system with main excitation frequencies observed as amplitude increase and phase fluctuation of signals during nonstationary rotor rotation speed (see example in Figure 17);
- Presence of nonharmonic signal components excited by wide bandwidth noise and turbulence which could be observed during specific flight conditions (see example in Figure 18).

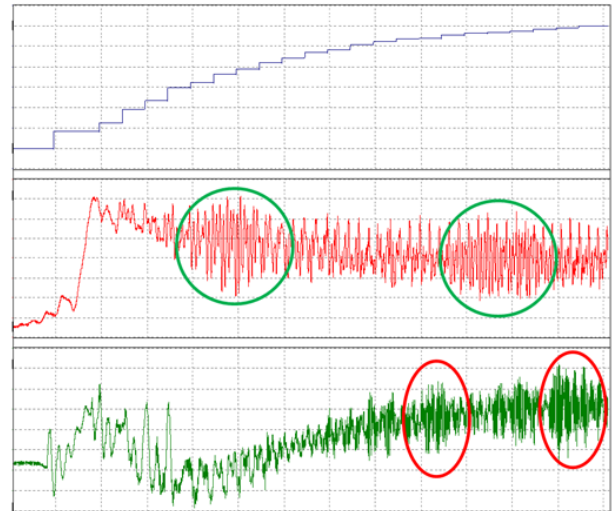


Figure 17. Engine start case measurements (top – rotor speed, mid – beamwise bending moment, bottom – chordwise bending moment, rounded – possible resonance between rotor and current excitation frequency).

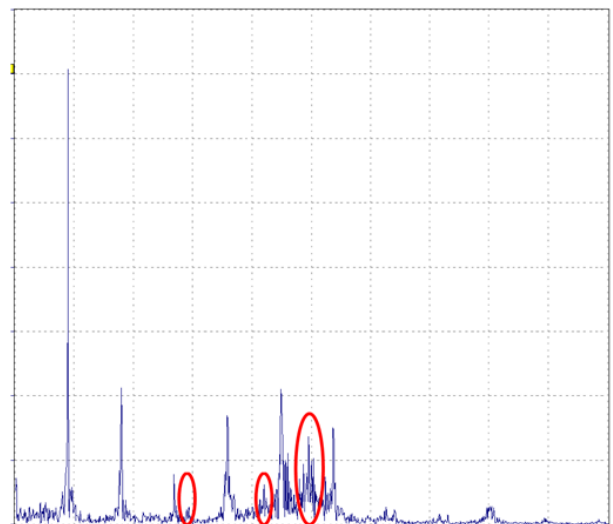


Figure 18. IGE Hover measurements – frequency spectrum of MR blade chordwise moment (rounded – frequencies where characteristic frequencies are excited)

### 5.3. MR blades tests on tied down helicopter.

The tied down PZL W-3 helicopter was used to perform first run of the MR with new blades. The engine start and stop together with ground idle to flight idle and back cases were used to retrieve possible excitation effect on signals characteristic. Every installed strain gauges section measured signal was analyzed separately using moving window DFT. Result of this analysis is registered as 2-D matrix of signal amplitude vs. time and frequency. Example result is presented in Figure 19.

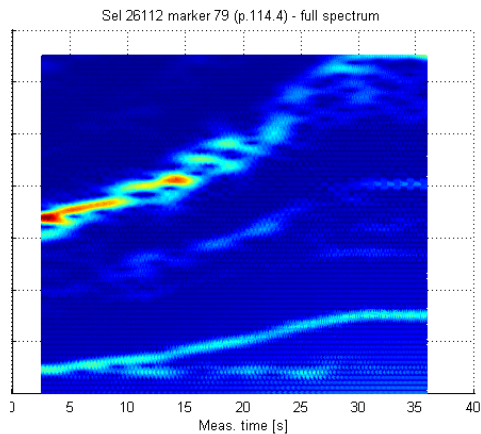


Figure 19. Example result of moving window procedure application on chordwise bending moment measured during MR speed increase from ground idle to flight idle.

The separately selected measured point is used as trace signal to retrieve first harmonic of MR speed vs time recorded during analyzed case. Example signal is presented in Figure 20.

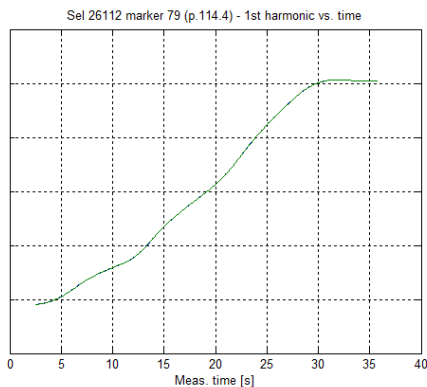


Figure 20. Example time plot of 1<sup>st</sup> harmonic retrieved from trace signal (MR shaft bending moment).

Retrieved 1<sup>st</sup> harmonic vs. time function allows to trace higher harmonic during particular event. All existing signals from blade strain gauges were combined and visualized as matrix of signals amplitude vs. frequency and blade radius. The polynomial interpolation was used for distribution of signals along blade.

The resulting bending/torsional moments distribution along blade was compared with equivalent variable for identified frequencies/mode shapes. Maximum similarity between measured and predicted load distribution shape is used as indicator of coincidence between natural mode and particular MR harmonics.

The example beamwise bending mode v2 identified signal is presented in Figures 21 - 23.

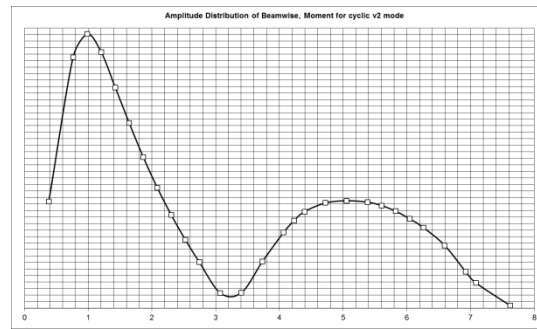


Figure 21. Predicted beamwise bending moment distribution for v2 mode.

Amplitude along the blade vs. frequency for 5<sup>th</sup> harmonic of MR rotational speed - vertical

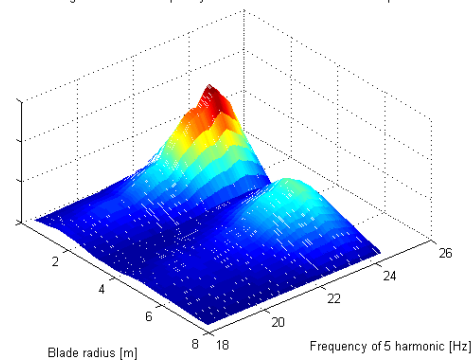


Figure 22. 3-D visualization of beamwise bending moment distribution present in signal during crossing with 5<sup>th</sup> MR harmonics.

Amplitude along the blade vs. frequency for 8<sup>th</sup> harmonic of MR rotational speed - vertical

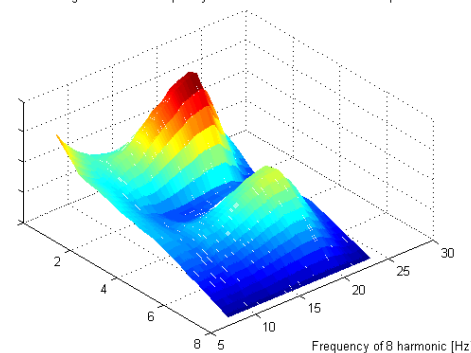


Figure 23. 3-D visualization of beamwise bending moment distribution present in signal during crossing with 8<sup>th</sup> MR harmonics.

The same procedure was repeated for all harmonics and measurement channels. Finally the verification of the Campbell diagram was performed. Comparison between predicted and identified from measurements frequencies is presented on Figure 24.

Identified Crossings Between Main Rotor Rotational Speed Harmonics and Rotor Natural Frequencies of the Blade

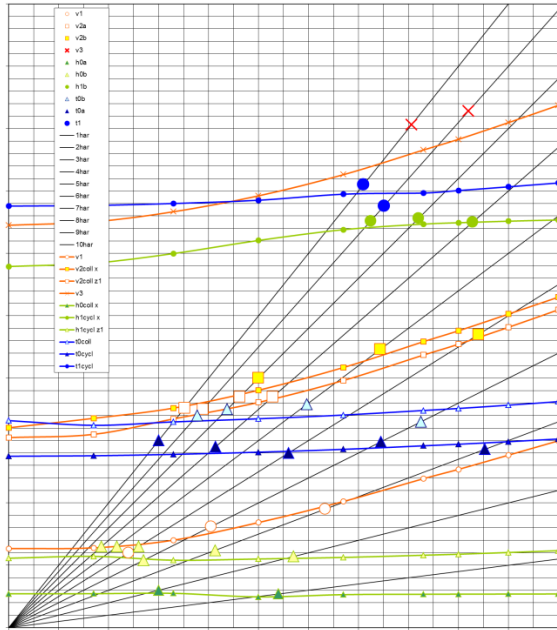


Figure 24. Comparison between predicted by Myklestad method and identified resonance frequencies from ground helicopter tests.

**5.4. MR blades tests in flight.**

Successful results of the ground tests allowed to start flight test campaign.

Prepared methodology for blade frequency identification was applied also for measurements performed during flights. Analyzes were performed also to find evidenced of characteristic frequencies in signals by removing narrow band harmonic part of frequencies corresponding to the harmonic loads.

This technique allows to emphasize part of signal belongs to the weak response on nonharmonic aerodynamic turbulence excitation – see Figures 25 - 26.

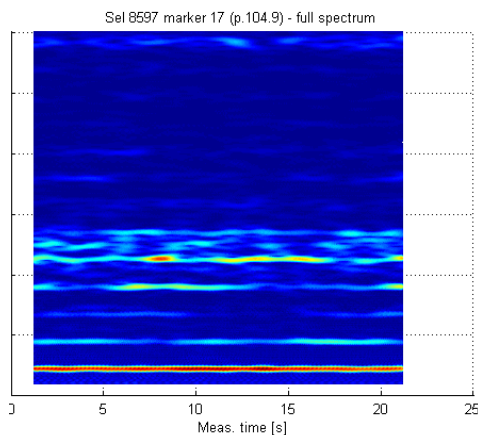


Figure 25. Moving window procedure applied to blade chordwise bending moment signal during hover.

Sel 8597 marker 17 (p.104.9) - harmonics removed

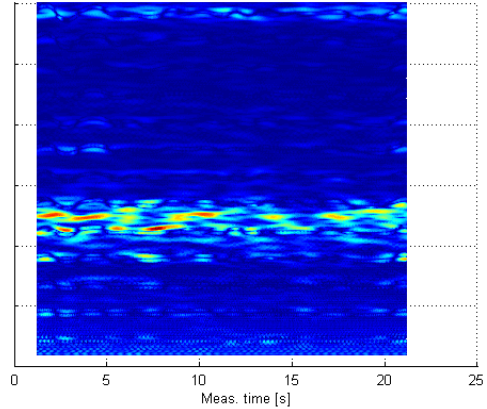


Figure 26. Moving window procedure applied to blade chordwise bending moment signal during hover with narrow bandstop filtering of harmonic signals.

Coupled analysis of every measured strain gauge along blade allowed estimating blade motion during flight and visualization of the loads distribution across the rotor surface.

Estimation of the blade deflection was based on simplified, uncoupled bending and torsion of the beam. Partial differential equation of bending and torsion was integrated in time to retrieve deflected shape of the blade. This method was used to animate rotor in flight with estimated deflection – see Figure 27.

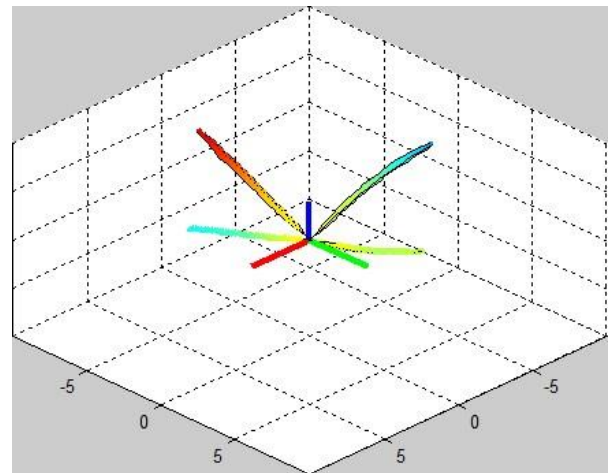


Figure 27. Snapshot of movie with visualization of PZL W-3A helicopter MR with new blades installed - blade deflection estimation in flight, color code proportional to the torsional deflection.



## 6. CONCLUSIONS

Following conclusions could be formulated as the summary of presented analyzes:

- Correct recognition of the modal properties of interface between rotor and helicopter fuselage and control system is crucial for proper prediction of rotor dynamics during rotor blade design stage;
- Measurements of rotor blade strains distribution along the blade allow retrieving excited rotor modes and could be used to validate rotor dynamics prediction done during design stage of rotor blades;
- Precise determination of phase angles between measured signals, taken into account during rotor dynamics identification procedure, allows proper recognition of the excited rotor blade modes;
- The simplified rotor blade models allow to predict rotor dynamics with satisfactory accuracy to assess which rotor blade modes are excited on helicopter

## 7. REFERENCES

- [1]. Weller W. H., Mineck R. E., *An Improved Computational Procedure for Determining Helicopter Rotor Blade Natural Modes*, NASA Technical Memorandum 78670 , NASA Langley Research Center, August 1978

---

### **Copyright Statement**

*The authors confirm that they, and/or their company or organization, hold copyright on all of the original material included in this paper. The authors also confirm that they have obtained permission, from the copyright holder of any third party material included in this paper, to publish it as part of their paper. The authors confirm that they give permission, or have obtained permission from the copyright holder of this paper, for the publication and distribution of this paper as part of the ERF proceedings or as individual offprints from the proceedings and for inclusion in a freely accessible web-based repository.*